Effect of the preparation methodology on some physical and electrochemical properties of Ti/Ir$_x$Sn$_{(1-x)}$O$_2$ materials

Josimar Ribeiro · Paula D. P. Alves ·
Adalgisa R. de Andrade

Abstract The aim of this work was to prepare electrodes based on the Ti/Ir$_x$Sn$_{(1-x)}$O$_2$ composition, as well as test their stability toward the chlorine evolution reaction (ClER). To this end, two different preparation routes were investigated: thermal decomposition of polymeric precursors (DPP) and standard decomposition using isopropanol as solvent (SD/ISO). A systematic investigation of the structural, morphological, and electrochemical properties of the anodes with a nominal composition of Ti/Ir$_x$Sn$_{(1-x)}$O$_2$, prepared through the two different methodologies, was carried out. The oxide layer surface morphology, microstructure, and composition were investigated by Energy Dispersive X-ray Spectroscopy (EDS) and Scanning Electron Microscopy (SEM) techniques prior to and after accelerated life tests. EDS analyses following total deactivation of the electrode gave evidence of a relatively large content of Ir in the coating. XRD results showed there was formation of solid solution between IrO$_2$ and SnO$_2$, and the degree of miscibility of these solutions is controlled by the preparation method. Thus, the DPP method led to phase separation and large interval of immiscibility between the oxides analyzed. On the other hand, the SD/ISO method led to formation of solid solution for all the investigated compositions. The SD/ISO method produced materials rich in Ir, so the electrode lifetime was much longer if compared with the DPP counterparts.

J. Ribeiro · P. D. P. Alves · A. R. de Andrade (✉)
Departamento de Química da Faculdade de Filosofia Ciências e
Letras de Ribeirão Preto, Universidade de São Paulo,
Av. Bandeirantes, 3900, Ribeirao Preto, SP 14040-901, Brazil
e-mail: ardandra@ffclrp.usp.br

Introduction

Dimensionally stable anodes (DSA®, patented by Diamond Shamrock Technologies S.A. Genebre—Swiss), which were introduced by Beer [1], exhibit good catalytic properties for chlorine-brine production and have been used in the industry since the 70s [2]. More recently, IrO$_2$ has been introduced to catalyze oxygen evolution in industrial electroplating processes [3]. The surface of these materials are very irregular and rough, and the porosity can be controlled by the conditions used in the preparation of the oxide [4]. In order to improve the electrocatalytic and mechanical properties of these anodes, different materials have been introduced in the composition of the oxide. The Ta$_2$O$_5$ is considered to a good material to promote mechanical stability, due to its outstanding behavior concerning passivation protection [5]. Therefore, the use of IrO$_2$–Ta$_2$O$_5$ electrodes has been proposed to overcome the low stability of the Ru–Ti oxide mixture [5–7]. Moreover, the introduction of SnO$_2$ into the anode coating has led to an improvement in both the electrocatalytic (better electronic conduction) and mechanical properties (substantial increase in the lifetime) of the electrode [8].

The thermal decomposition of chloride salts dissolved in acid medium (HCl 1:1 v/v) is a standard method that is generally used in the preparation of DSA®-types electrodes. This method has been used since the pioneering work of Beer [1, 9–11], and the oxide deposit is produced under relatively high temperatures (400–600 °C) by firing thin layers of the precursor solution until the desired oxide loading is achieved. The simplicity of this method has made it very popular for the production of oxide coatings; however, the use of volatile precursors like tin salts results in failure of the standard preparation [12]. The major problem concerning the preparation of electrodes containing Sn by

thermal decomposition is the proper control of SnO_2 content in the coating. This is because $SnCl_4$ volatilization takes place at temperatures higher than 114 °C [12, 13]. Tin loss values as high as 50% have been reported [9, 14]. Based on these findings, careful control of the preparation method is important to maintain the desirable SnO_2 content. Therefore, an alternative preparation method based on the decomposition of polymeric precursor (DPP) has been proposed, in order to overcome the problem of Sn volatilization. In this method, the Sn-atom can be fixed in the polyester chain formed during the resin preparation [8, 15], so that a better control of the metal oxides present in the ceramic coating can be obtained [8, 16]. It has also been reported that Ti/RuO_2 and Ti/IrO_2 electrodes prepared by the DPP method exhibit improved electrochemical performance; i.e., longer lifetime and higher electrochemical active area than those prepared by standard methods [8, 17–19]. Another approach that has been investigated is changing the solvent used in the standard decomposition (SD). In this way, isopropanol (SD/ISO) has proven to be a good alternative to acid water [12].

In our laboratory we have investigated different compositions and preparation methods for the obtainment of oxides electrodes. We have found out that the electrochemical and structural properties of theses materials change depending on the preparation route [8, 12]. In the present study we report results for binary $Ti/Ir_xSn_{(1-x)}O_2$ compositions obtained by two different method (SD/ISO and DPP). We also report the morphological and electrochemical characterization of the obtained electrodes, as well as their performance as anodes for ClER.

Experimental

Electrodes preparation

$Ti/Ir_xSn_{(1-x)}O_2$-DPP electrodes ($x = 0.1$; 0.3; 0.5; 0.7 and 0.9) were prepared by thermal decomposition ($T_{calcination}$: 450 °C). The solution of the polymeric precursors were prepared by mixing citric acid (CA) (Merck) in ethylene glycol (EG) (Merck) at 65 °C. After total CA dissolution, the temperature was raised to 90 °C and tin citrate (TC), prepared as described elsewhere [15], was then added. The molar ratio CA:EG:Sn was 3:10:1. Iridium was introduced into the mixture by adding an appropriate amount of 0.2 mol dm^{-3} $IrCl_3.nH_2O$ (Aldrich) solution dissolved in HCl 1:1 (v/v). The precursor mixtures were applied by brushing on both sides of the pretreated Ti support [8]. After application of each coating, the electrode was heated in an air oven at 100 °C for 5 min to allow polymerization, and it was then calcined at 450 °C for 5 min. Averages of 8–10 applications were required to obtain the desired oxide

loading (2 μm) corresponding to ~3.0 mg cm^{-2}. The layers were finally annealed for 1 h under oxygen flux of 5 dm^3 min^{-1}. Duplicate samples were prepared for each electrode composition. Details of the preparation and the final mounting of the electrodes are described elsewhere [20].

Nominal compositions of $Ti/Ir_xSn_{(1-x)}O_2$-SD/ISO electrodes ($x = 0.1$; 0.3; 0.5; 0.7 and 0.9) were prepared at the same firing temperature described above (450 °C), using an appropriate amount of the precursor solutions of $IrCl_2.nH_2O$ (Aldrich) and $SnCl_2$ (Merck) dissolved in isopropanol (Merck).

Morphological characterization

Powders annealed at 450 °C for 5 h of DPP and SD/ISO samples were prepared for XRD experiments. X-ray analysis was performed by means of a Model D5005 Siemens instrument using CuK_α radiation ($\lambda = 1.5406$ Å). The following parameters were kept constant during X-ray analysis: 2θ range = 20°–85°, step = 0.03°, step time = 5 s, total analysis time = 1.8 h, and temperature = 27 °C.

Cell parameters were obtained by a computer program, which calculated the unit cell parameters using the least squares method. Experimental 2θ and reflection parameters (hkl) were used as a first guess to obtain the unit cell parameter: a = b = 4.4983 and c = 3.1544 for IrO_2, and a = b = 4.7382 and c = 3.1871 for SnO_2. The analysis of the relevant position of IrO_2–SnO_2 to the $K_{\alpha1}$ monochromatic radiation was obtained by fitting the experimental angular range of interest to the pseudo-Voigt 1 function per crystalline peak plus a background with the aid of a computer refinement program (Profile Plus Executable—version 2.0—1995 Siemens AG).

The detectable reflections (110), (101), (200), and (211) were used for the determination of the cell parameters of the solid solution phase. The values of crystallite size were obtained through the Scherrer equation [21]:

$$D = 0.9 \times \lambda/\beta \times \cos \theta_\beta \qquad (1)$$

where D is the average dimension of the crystallites perpendicular to the reflecting planes; λ is the radiation wavelengtht of the (1.5406 Å); β is the reflection width at half-maximum intensity measured in radians, and θ_β is the angle at the maximum intensity.

Surface morphology, microstructure, and elemental composition of the deposited oxide films were analyzed through scanning electron microcopy (SEM) and energy dispersive X-ray spectroscopy (EDS) using a Leica-Zeiss LEO 440 model SEM coupled to a Oxford 7060 model analyzer and a Zeiss 940 microscope coupled to a ZAF 4FLF link Analytical system.

Cell and equipment

The electrochemical studies were performed using $2.99 \ mol \ dm^{-3} \ NaCl + 0.01 \ mol \ dm^{-3} \ HCl$ as the supporting electrolyte. Water was purified in a Millipore-Milli-Q apparatus. All solutions were deaerated before and during each experiment by using suprapur nitrogen (White Martins). All electrochemical experiments were carried out at room temperature.

A three-compartment cell was used throughout the experiments and consisted of: (i) a main body (~100 mL), (ii) two smaller compartments containing two platinized platinum wires (15 cm) as counter electrodes, which were isolated from the main body by coarse glass frits. The KCl saturated calomel electrode (SCE) was used as the reference.

The accelerated life test (ALT) was performed under galvanostatic condition ($400 \ mA \ cm^{-2}$) in chlorine solution ($NaCl \ 2.99 \ mol \ dm^{-3} + HCl \ 0.01 \ mol \ dm^{-3}$) at room temperature. The electrodes were considered inactive for ClER when the potential of the working electrode reached 6 V. All experiments were repeated at least twice.

Electrochemical measurements were carried out using an AUTOLAB (PGSTAT 30) potentiostat/galvanostat coupled by a computer. Freshly prepared electrodes were activated by cycling the potential between +0.0 and +0.9 V vs. SCE for 50 cycles. This procedure furnished a steady state condition for voltammetric curves (CV) recorded in the investigated potential range (+0.0 and +0.9 V vs. SCE). The anodic voltammetric charge (q^*) was determined by integration of the anodic region of the i versus E curve between +0.0 and +0.9 V vs. SCE.

Results and discussion

XRD measurements and surface morphology

Figure 1 shows the XRD-pattern of different compositions of IrO_2 and SnO_2 samples prepared by both methods, obtained by firing mixture of precursors at 450 °C for 5 h. Two phases can be observed in the case of samples prepared by DPP (Fig. 1a); one is attributed to IrO_2 and the other to SnO_2. The observed IrO_2 and SnO_2 peaks show reflections related with the rutile structure (110, 101, 200, and 211), with space group P42/mnm [22]. This result differs from that reported by Profeti et al. [18] for thin films of $Ir_{0.3}Sn_{(0.7-x)}Ti_xO_2$ prepared in a similar way. In that case, only the presence of SnO_2 with a cassiterite structure was observed. On that occasion, the authors suggest that the identification of IrO_2 was hindered by the proximity between the SnO_2 and TiO_2 peaks.
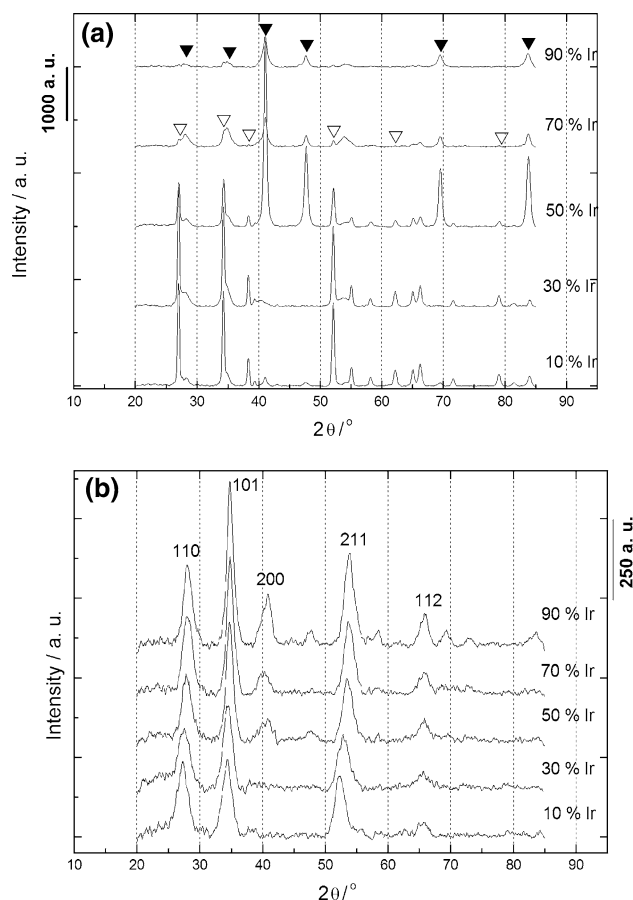
Fig. 1 XRD-pattern of the powder of $Ir_xSn_{(1-x)}O_2$ mixtures prepared through the DPP (**a**) and SD/ISO (**b**) methods. $T_{calc.}$ = 450 °C, O_2 flux = 5 $dm^3 \ min^{-1}$ for 5 h. (▼) IrO_2 [JCPDS—43-1019] and (▽) SnO_2 [JCPDS—41-1445]

Deconvolution of the peaks in the XRD of the iridium-tin oxide mixture of the DPP-samples (Fig. 1a) was performed as described elsewhere [23]. By comparing the positions obtained with the respective pure oxides [22], it is possible to confirm the presence of two saturated solid solutions. Powders containing a higher concentration of one of the oxides exhibit a reciprocal solubility of either IrO_2 or SnO_2. However, the observed miscibility is quite low (10%), even if one considers that these oxides satisfy the Hume-Rothery rule [24] condition for the formation of substitutional solid solution; i.e., same valence (+4) and small difference between the ionic radii of the two metals (0.063 nm Ir^{4+} and 0.069 nm Sn^{4+}) [25].

Figure 1b shows the XRD-pattern of the samples prepared by the SD/ISO method. Contrary to the DPP-samples, there is formation of solid solution for all the investigated compositions exhibiting the rutile structure. This shows that the preparation method plays an important role in the final composition and structural form of the desired material. In this particular case, the SD/ISO method
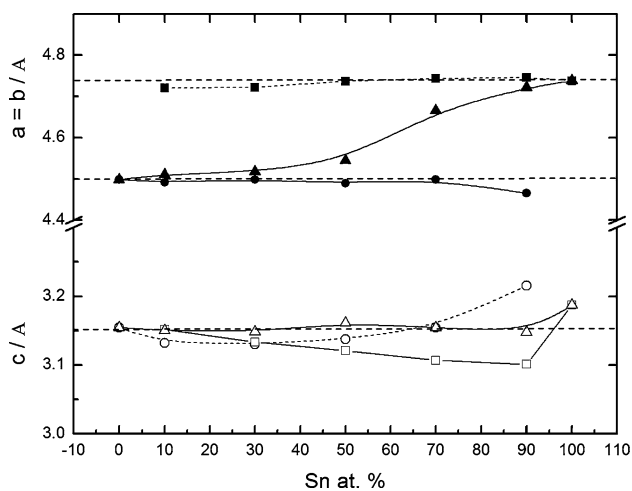
Fig. 2 Unit cell parameters for the $Ir_xSn_{(1-x)}O_2$ system as a function of the Sn content. Open symbols (c), close symbols (a and b). DPP: (■ and □) SnO_2 samples saturated with Ir and (● and ○) IrO_2 samples saturated with Sn; SD/ISO: (▲ and △) solid solution of IrO_2–SnO_2

favored the substitution of Ir and Sn atoms in their respective crystalline reticules. Thus, Sn-rich compositions display peaks shifted toward the pure SnO_2 pattern, indicating that Ir atoms may be incorporated into the SnO_2 crystalline reticule. The opposite trend is observed for Ir-rich samples, which have their peaks shifted toward the pure IrO_2 pattern due to the incorporation of Sn atoms into the IrO_2 crystalline reticule.

Figure 2 shows the unit cell parameters for the tetragonal phase for all the oxides prepared in this work. This figure confirms the structural changes depending on the preparation methodology. In fact, it can be observed that in the case of the samples prepared by SD/ISO, the a/b parameter shifts away from the theoretical values with increasing concentration of one oxide over the other. For the Ir-rich samples, the unit cell parameters shift toward the theoretical value of pure IrO_2. The opposite happens with Sn-rich samples. This is a typical evidence of substitutional solid solution formation. Moreover, the c parameter does not change as a function of the composition suggesting that the substitution of the metals occurs in the a/b plane of reticule.

On the other hand, for the DPP samples, there is small variation in the a/b parameter and a wide variation in the c parameter, if compared with the theoretical values. This indicates the formation of an interstitial saturated solid solution.

Tables 1 and 2 show the D-values obtained for the investigated IrO_2–SnO_2 samples prepared through of the DPP route. It can be observed that the D-values are higher for the SnO_2 saturated solid solutions (10–25 nm) if compared with the IrO_2 (3.5–13 nm) ones. As stated before [23, 24], the crystallite size changes with the crystallographic

Table 1 Crystallite size obtained for the IrO_2 phase prepared by the DPP route. T_{cal} = 450 °C, for 5 h

Ir % at.	D/Å				
	110	101	200	211	301
10	69	98	–	59	–
30	42	87	35	59	–
50	71	66	59	51	117
70	40	51	59	61	130
90	78	66	77	–	76

Table 2 Crystallite size obtained for the SnO_2 phase prepared by the DPP route. T_{cal} = 450 °C, for 5 h

Sn % at.	D/Å				
	110	101	200	211	301
10	132	250	–	191	–
30	169	111	–	153	100
50	129	156	170	149	–
70	202	154	207	158	119
90	196	174	185	166	134

Table 3 Crystallite size obtained for the $Ir_xSn_{1-x}O_2$ solid solution prepared by the SD/ISO route. T_{cal} = 450 °C, for 5 h

Ir % at.	D/Å				
	110	101	200	211	112
10	26	33	–	45	–
30	27	46	–	53	31
50	34	52	41	45	34
70	42	51	60	43	46
90	39	52	52	35	83

direction which suggests a non-equiaxial growth of the particles.

Table 3 shows the D-values obtained for the solid solution of IrO_2–SnO_2 prepared by the SD/ISO method as a function of the loaded Ir. The crystallite size obtained for this material ranges from 2.6–8.3 nm and is smaller if compared to the crystallite size of the same composition prepared by DPP.

SEM and EDS analyses of thin films

Figure 3 show some representative micrographs of $Ti/Ir_xSn_{(1-x)}O_2$ films prepared by both methodologies, before (a and b) and after the accelerated life test, ALT (c and d). The surface morphology of the films is typical of thermally prepared oxides [6, 8, 12, 26]. All the investigated compositions were rough and some of them showed

Fig. 3 Representative SEM image of Ti/Ir$_{0.5}$Sn$_{0.5}$O$_2$ electrodes prepared through the DPP (**a** and **c**) and SD/ISO (**b** and **d**) method. Before (**a** and **b**) and after (**c** and **d**) ALT. Conditions: $i = 400$ mA cm^{-2}; 2.99 mol dm^{-3} NaCl + 0.01 mol dm^{-3} HCl
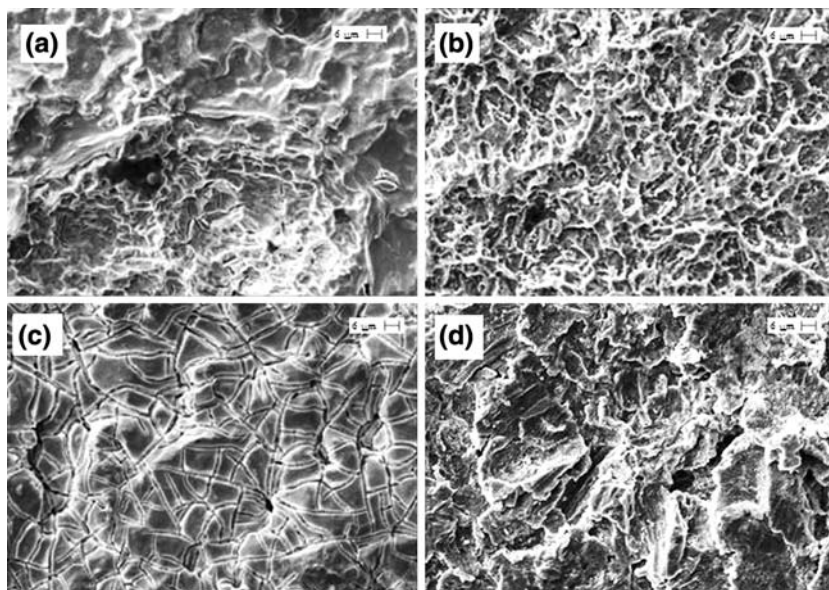
visible small cracks (2–7 μm) that were present mostly in samples prepared through SD/ISO route. After ALT, the thin films surface became smoother, indicating that there was some erosion/corrosion of the material. In fact, roles can be seen on the surface of the material.

Figure 4 shows the Ir$_{experimental}$ atom % as a function of the Ir$_{nominal}$ atom % obtained by EDS focused on the electrode surface for both investigated preparation methods, before and after the ALT. By comparing the nominal and experimental values, one can observe that electrodes prepared by the DPP method are Sn-rich, while those prepared by SD/ISO are Ir-rich. The enrichment of electrodes prepared through the DPP route in tin had been observed by one of us [8] before for Ti/Ru$_{0.3}$Sn$_{(0.7-x)}$Ti$_x$O$_2$ mixtures. This method is very interesting when one wants to obtain the final film more homogeneously distributed. Recently, a very close correlation between nominal and experimental tin and iridium concentrations was reported by Profeti et al. [18] for ternary electrodes prepared by the polymeric precursor method.

The lower tin content observed in the SD/ISO electrode can be explained by the fact that SnCl$_4$ volatilization makes it difficult to efficiently hold tin atoms during the calcinations process [12]. Low Sn-content is frequently found in the literature, for example, in the work of Lassali et al. [14], they observed huge volatilization of the tin content if compared with the nominal composition for tin and iridium oxide prepared using HCl as solvent. Other methods such as sol–gel [19] were also able to enhance the tin content in the catalyst mixture. The amount of tin recovery at the end of the firing process is equivalent to that obtained by us using the SD/ISO method; however, the reproducibility of the sol–gel process is much more laborious and expensive.
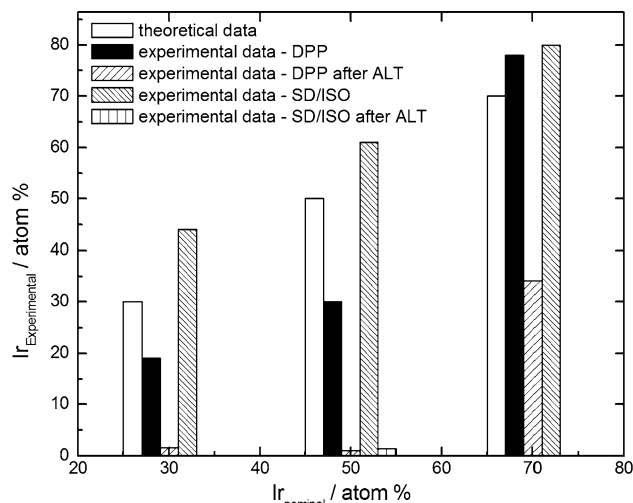
Fig. 4 Ir$_{experimental}$ atom % as a function of Ir$_{nominal}$ atom % for Ti/Ir$_x$Sn$_{(1-x)}$O$_2$ electrodes. Experimental data before and after ALT ($i = 400$ mA cm^{-2}, 2.99 mol dm^{-3} NaCl + 0.01 mol dm^{-3} HCl)

Table 4 shows the ALT-values obtained for the Ti/Ir$_x$Sn$_{(x-1)}$O$_2$ system prepared by both methods. One can observe that the service life of the electrodes prepared by the SD/ISO method is considerable higher (~40%) than that of the one prepared by the DPP route.

The amounts of iridium observed for the Ti/Ir$_{0.5}$Sn$_{0.5}$O$_2$ nominal composition for example, before and after the ALT, are as follows: for the DPP route, the composition changes from Ir$_{0.2}$Sn$_{0.4}$Ti$_{0.4}$ to Ir$_{0.01}$Sn$_{0.02}$Ti$_{0.91}$. In the case of SD/ISO route, changes from Ir$_{0.33}$Sn$_{0.2}$Ti$_{0.47}$ to Ir$_{0.01}$Sn$_{0.01}$Ti$_{0.98}$. By comparing the EDS data, one can conclude that iridium and tin leaches from the coating of both electrodes. Therefore, a considerable increase in the

Table 4 Lifetime values obtained for the $Ti/Ir_xSn_{(1-x)}O_2$ electrodes as a function of the composition and preparation method. $T_{cal} = 450$ °C, $\phi = 2$ μm, $i = 400$ mA cm^{-2}, SE = 2.99 mol dm^{-3} NaCl + 0.01 mol dm^{-3} HCl

Nominal composition	Lifetime (h)	
	DPP	SD/ISO
$Ti/Ir_{0.3}Sn_{0.7}O_2$	152	175
$Ti/Ir_{0.5}Sn_{0.5}O_2$	35	>250
$Ti/Ir_{0.7}Sn_{0.3}O_2$	58	200

titanium signal is observed. The Ti observed for freshly prepared electrodes may be due to Ti-support once the sampling depth of the EDS might, in some cases, be comparable to or even larger than the oxide film thickness. After the ALT, the increase in the Ti signal is probably caused by a decrease in the thickness of the catalytic layer due to material loss, which may be attributed to erosion/corrosion process.

Electrochemical characterization

Figure 5 shows the cyclic voltammogram obtained in 2.99 mol dm^{-3} NaCl + 0.01 HCl mol dm^{-3}. The cyclic voltammograms show a large peak typical of the Ir(III)/Ir(IV) redox transition located in the region between at +0.4 and +0.8 V/SCE. However, electrodes prepared by the SD/ISO method display a more defined peak.

Some studies using iridium–tin oxide electrodes in chloride medium can be found in the literature, but the observed Ir(III)/Ir(IV) solid state transition is similar to that obtained in neutral medium (NaClO$_4$ 1.0 mol dm^{-3}) [26] and acid [19, 27–31].

Table 5 shows a set of electrochemical parameters obtained for this system. It is possible to see that its behavior depends on the investigated preparation route. An increase in q* and roughness factor (RF), obtained as described elsewhere [18, 26], is observed for DPP electrodes. This is the expected behavior when one increases the catalytic oxide (Ir) loading. In fact, similar results have also been reported for IrO$_2$–SnO$_2$ electrodes prepared in acid medium [31]. On the other hand, SD/ISO materials display an unexpected behavior, with a decrease in q* when the iridium content is enhanced. Macroscopically, there is not much difference between the morphology of the SD/ISO electrodes that could justify this behavior. However, the crystallite size increases for high tin content samples.

The current efficiency for chlorine production was measured at a fixed potential (1.05 V/SCE). There is not a direct correlation between current efficiency and morphological factor (total charge and RF). In fact, the DPP electrodes are twice more efficient at generating chlorine
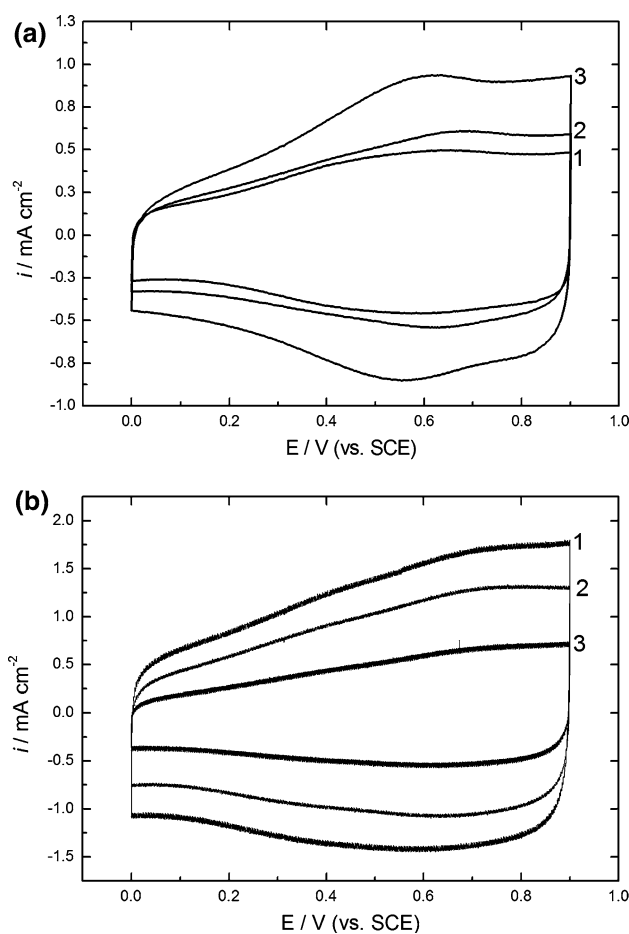
Fig. 5 Cyclic voltammograms as a function of the IrO$_2$ content in $Ti/Ir_xSn_{(1-x)}O_2$ electrodes (**a**) $Ti/Ir_xSn_{1-x}O_2$—SD/ISO; (**b**) $Ti/Ir_xSn_{1-x}O_2$—DPP. (1) $Ti/Ir_{0.3}Sn_{0.7}O_2$; (2) $Ti/Ir_{0.5}Sn_{0.5}O_2$; (3) $Ti/Ir_{0.7}Sn_{0.3}O_2$. SE = 2.99 mol dm^{-3} NaCl + 0.01 mol dm^{-3} HCl; n = 20 mV s^{-1}; A = 2 cm^2; $T_{calc.}$ = 450 °C

Table 5 Voltammetric charge (q*), roughness factor (RF), current efficiency (E = 1.05 V/SCE) and normalized current density of $Ti/Ir_xSn_{(1-x)}O_2$ electrodes as a function of the oxide composition and preparation method

	Electrode composition	q* (mC/cm^2)	RF	i (mA/cm^2)	i/q*
DPP	$Ti/Ir_{0.3}Sn_{0.7}O_2$	16.8	512	11.1	0.7
	$Ti/Ir_{0.5}Sn_{0.5}O_2$	19.5	687	11.4	0.6
	$Ti/Ir_{0.7}Sn_{0.3}O_2$	29.7	912	10.4	0.4
SD/ISO	$Ti/Ir_{0.3}Sn_{0.7}O_2$	61.7	750	5.2	0.1
	$Ti/Ir_{0.5}Sn_{0.5}O_2$	41.8	462	8.0	0.2
	$Ti/Ir_{0.7}Sn_{0.3}O_2$	19.4	225	7.0	0.4

than the SD/ISO ones. This indicates that, besides the area factor, intrinsic electronic activation of the material may play a more important role in the catalysis of the reaction. In the case of the DPP method, a more controlled distri-

bution of the metal atoms in the polymeric chain can fix these atoms and may contribute to a steadier surface during the thermal loading treatment. This might promote a structure that favors an increase in the inter-grain region conductivity [32].

Conclusion

Both method investigated in this work have proven to be good alternatives for fixing tin atoms in IrO_2–SnO_2 electrodes prepared through the thermal decomposition route, especially if compared with other methodologies reported in the literature; e.g., sol–gel and SD/HCl.

XRD-data showed that the size and structure of the crystallites depend on the preparation method used. Moreover, the electrode lifetime for SD/ISO electrodes is much longer if compared with their counterpart prepared by the DPP method, which may be mainly attributed to the differences in the porosity of the ceramic material and solid solution formatted.

The DPP method furnishes an Sn-rich electrodes, whereas SD/ISO promotes Ir enrichment of the coatings. Considering the chlorine evolution reaction, the DPP materials are twice more efficient than the SD/ISO ones. This advantage outweighs the serious drawback of shorter lifetime and may open the possibility of using this material under mild oxidations condition for the treatment of organic waste in water treatment.

References

1. Beer HB (1966) U. S. Patent. New York 3:199
2. Trasatti S (2000) Electrochim Acta 45:2377
3. Morimitsu M, Otogawa R, Matsunaga M (2000) Electrochim Acta 46:401
4. Trasatti S, Lodi G (1981) In: Trasatti S (ed) Electrode of conductive metallic oxides, part A. Elsevier, Amsterdam, p 521
5. Comninellis C, Vercesi GP (1991) J Appl Electrochem 21:335
6. Ribeiro J, De Andrade AR (2004) J Electrochem Soc 151:D106
7. Ardizzone S, Bianchi CL, Cappelletti G, Ionita M, Minguzzi A, Rondinini S, Vertova A (2006) J Electroanal Chem 589:160
8. Forti JC, Olivi P, De Andrade AR (2001) Electrochim Acta 47:913
9. Comninellis C, Vercesi GP (1991) J Appl Electrochem 21:136
10. Ortiz PI, De Pauli CP, Trasatti S (2004) J New Mater Electrochem Syst 7:153
11. Roginskaya Y, Goldstein M, Morozova O, Glazunova L, Russ (2001) J Electrochem 37:1065
12. Coteiro RD, Teruel FS, Ribeiro J, De Andrade AR (2006) J Braz Chem Soc 17:771
13. Handbook of chemistry and physics, 55th edn. C.P. INC. 1974–75, Clevend, Ohio
14. Lassali TAF, Bulhões LOS, Abeid LMC, Boodts JFC (1997) J Electrochem Soc 144:3348
15. Pechini MP, Adams N (1967) US Patent, 3,330,697:1
16. Olivi P, Pereira EC, Longo E, Varella JA, Bulhões LOS (1993) J Electrochem Soc 14:L81
17. Terezo AJ, Pereira EC (1999) Electrochim Acta 44:4507
18. Profeti D, Lassali TAF, Olivi P (2006) J Appl Electrochem 36:883
19. Lassali TAF, Boodts JFC, Bulhoes LOS (2000) J Non-Crystalline Solids 273:129
20. Garavaglia R, Mari CM, Trasatti S (1984) Surf Technol 23:41
21. Cullity BD (1978) Elements of X-ray diffraction. Addison-Wesley, California, p 102
22. Powder Diffraction File in: Joint Committee on Powder Diffraction Standards, International Center for Diffraction Data. 1996: Pennsylvania. PDF-file: 43-1019 for IrO_2 and 41-1445 for SnO_2
23. Nanni L, Polizzi S, Benedetti A, De Battisti A (1999) J Electrochem Soc 146:220
24. Callister WD (1999) Materials science and engineering, 5a edn. John Wiley & Sons, USA
25. Huheey JE, Keiter EA, Keiter RL (1933) Inorganic chemistry—principles of structure and reactivity, 4th edn. HarperCollins, New York, USA
26. Alves PDP, Magali S, Tremiliosi-Filho G., De Andrade AR (2004) J Braz Chem Soc 15:626
27. Zanta CLP, De Andrade AR, Boodts JFC (2000) J Appl Electrochem 30:467
28. Zanta CLP, De Andrade AR, Boodts JFC (1999) Electrochim Acta 44:3333
29. Marshall A, Børresen B, Hagen G, Tsypkin M, Tunold R (2006) Electrochim Acta 51:3161
30. Vázquez-Gómez L, Horváth E, Kristóf J, Rédey A, De Battisti A (2006) Appl Surf Sci 253:1178
31. Lassali TAF, Boodts JFC, Bulhões LOS (2000) J Appl Electrochem 30:625
32. Loucka T (1977) J Appl Electrochem 7:211